

Personalized treatment with retigabine for pharmacoresistant epilepsy arising from a pathogenic variant in the KCNQ2 selectivity filter

Andreea Nissenkorn^{1,2,3}, Polina Kornilov⁴, Asher Peretz⁴, Lubov Blumkin^{2,3}, Gali Heimer^{1,3}, Bruria Ben-Zeev^{1,3}, Bernard Attali⁴

¹ Pediatric Neurology Unit, Edmond and Lilly Safra Pediatric Hospital, Chaim Sheba Medical Center, Tel Ha Shomer, Israel

² Pediatric Neurology Unit, Edith Wolfson Medical Center, Holon, Israel

³ Pediatric Department, The Sackler School of Medicine, Tel Aviv University, Tel Aviv, Israel

⁴ Physiology Department, The Sackler School of Medicine, Tel Aviv University, Tel Aviv, Israel

Received November 23, 2020;
Accepted May 01, 2021

This work was presented as a poster at the European Pediatric Society Meeting 4/2019, Athens

ABSTRACT

Objective. Mutations in the *KCNQ2* gene, encoding the voltage-gated potassium channel, Kv7.2, cause neonatal epilepsies. The potassium channel opener, retigabine, may improve epilepsy control in cases with loss-of-function mutations, but exacerbate seizures in cases with gain-of-function mutations. Our aim was to describe a patient with a *KCNQ2* mutation within the K⁺-selectivity filter and illustrate how electrophysiological analysis helped us to implement personalized treatment.

Methods. Medical history of a patient with severe neonatal epileptic encephalopathy was recorded. Diagnosis was reached by whole-exome-sequencing. The pathogenic variant was expressed in Chinese hamster ovary cells, and patch-clamp studies were performed, directing therapy.

Results. A seven-year-old male presented with neonatal seizures, progressing to hundreds of seizures/day without developmental milestones. Whole-exome sequencing revealed a pathogenic variant, p.Gly281Arg, in the *KCNQ2* gene, located within the ion selectivity filter of the pore, predicted to cause loss-of-function of Kv7.2, not affected by retigabine. Patch-clamp analysis revealed no current with the mutant homomer and reduced current with heterotetramer (*KCNQ2*^{WT}/*KCNQ2*^{G281R}/*KCNQ3*^{WT}) channels, consistent with a dominant-negative effect. Addition of 5 μM retigabine did not produce a current with the mutant homomer, but increased current with the heterotetramer (V₅₀: -30.4 mV vs. -51.3 mV). Following these results, retigabine at 15 mg/kg was administered off-label, prompting a 90% seizure reduction. Drug withdrawal, imposed by revocation of marketing authorisation for retigabine, caused 50% increase in seizure burden.

Significance. Retigabine may be used for precision therapy in patients with *KCNQ2*-related epilepsy due to loss-of-function variants. It is imperative to reintroduce safe marketing of retigabine for selected patients as personalized treatment.

Key words: antiepileptic drugs, epileptic encephalopathy, patch-clamp analysis, precision medicine, neonatal seizures

• **Correspondence:**
Andreea Nissenkorn
Pediatric Neurology Unit,
Edith Wolfson Medical Center,
Holon, Israel
<andreean@wmc.gov.il>

The neuronal M channels, belonging to the voltage-gated potassium channel Kv7 family, have emerged as critical players in epilepsy [1, 2]. Assembled as heterotetramers of Kv7.2 and Kv7.3 subunits, M channels generate subthreshold, non-inactivating voltage-gated K⁺ currents that play an important role in controlling neuronal excitability [1, 3-7]. Pathogenic variants in the *KCNQ2* gene, encoding for the Kv7.2 channel subunit, were initially linked to benign familial neonatal epilepsy [8, 9], but later were also associated with early-onset epileptic encephalopathy with cognitive disability and suppression-burst on EEG (electroencephalogram) [10, 11]. Electrophysiological studies have demonstrated a correlation between the extent of loss-of-function caused by protein altering variants and clinical severity [12-16]. Recently, gain-of-function variants, causing a distinct phenotype of epileptic encephalopathy without neonatal seizures, were also described [17, 18].

The Kv7.2 channel opener, retigabine (RTG) (ezogabine), was developed as an antiepileptic drug, suppressing seizures in animal models as well as in patients, due to a general effect on neuronal excitability [19, 20]. RTG acts as a positive allosteric modulator of M channels. It binds to a hydrophobic pocket near the channel gate and interacts with a tryptophan residue at the S5 segment to stabilize the open state of the channel, therefore increasing the number of M channels that are open at rest [21]. It is therefore expected that acute application of RTG will decrease intrinsic neuronal excitability as well as the spontaneous firing rate. In cases with loss-of-function pathogenic variants in the *KCNQ2* gene, RTG may have a positive effect [11, 22, 23], but for gain-of-function mutations, seizures are expected to be aggravated by treatment [17, 18].

In this study, we describe a patient with a *KCNQ2* pathogenic variant, p. Gly281Arg, located within the pore K⁺-selectivity filter. Patch-clamp analysis revealed that this pathogenic variant causes a loss of function, and helped us in directing an antiepileptic treatment.

Materials and methods

The medical history of a patient with severe neonatal epileptic encephalopathy was recorded. Diagnosis was reached by performing whole-exome sequencing. The effect of the protein altering variant was assessed in Chinese hamster ovary (CHO) cells by patch-clamp studies, in order to aid in directing drug therapy.

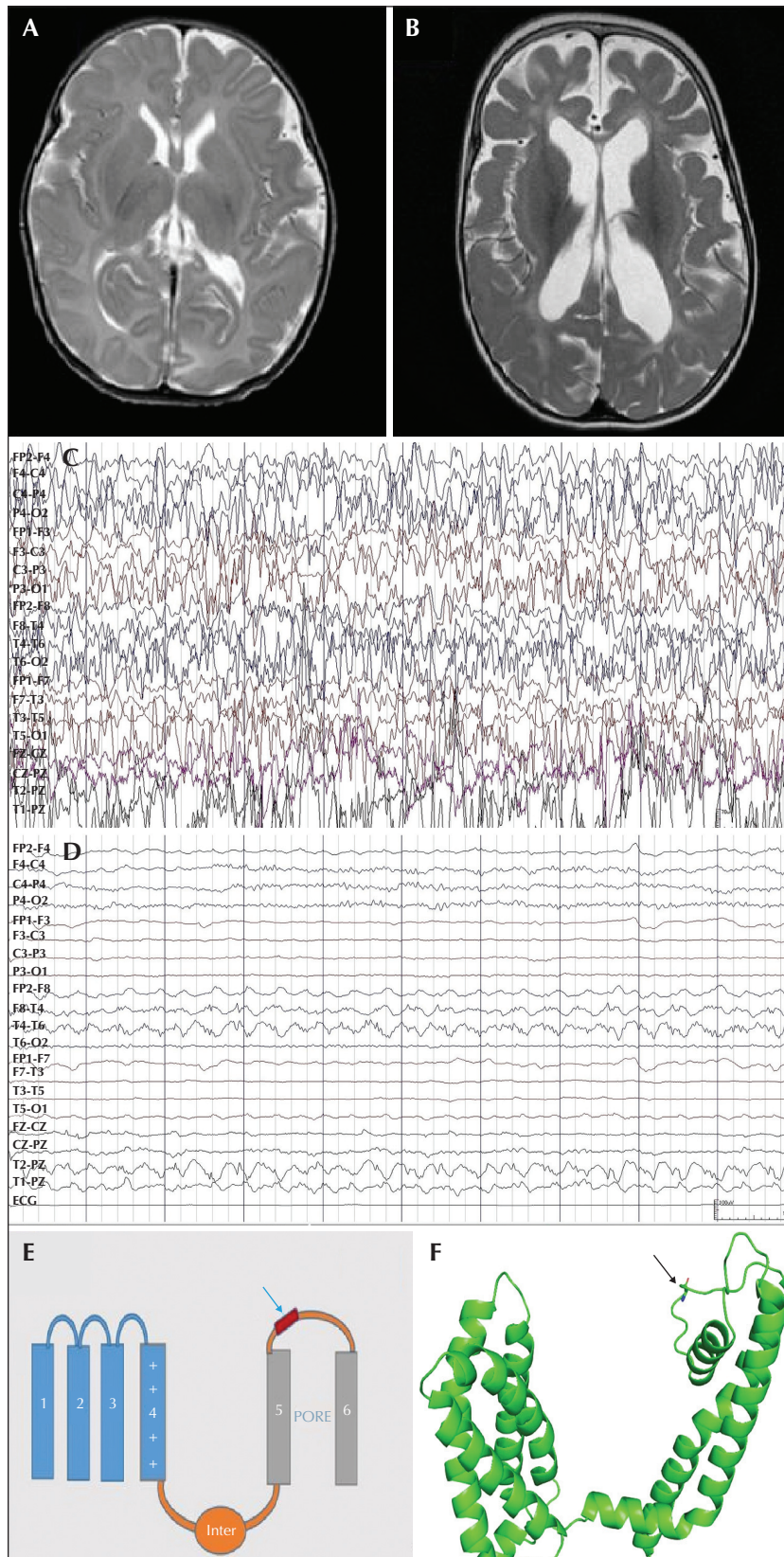
Molecular and bioinformatics studies

DNA was extracted from peripheral blood after written legal consent, according to the Ethical Committee of

the Sheba Medical Center, IRB 7786-10. Trio whole-exome sequencing was performed at the Center for Human Genome Variation, Duke University School of Medicine, Durham, North Carolina, USA, as a part of a research project endeavouring genetic diagnosis of 119 patients with various neuro-metabolic phenotypes [24]. The coding regions were extracted with the 65-Mb Illumina TruSeq Exome Enrichment Kit (Illumina, San Diego, CA), and sequenced using the HiSeq 2000 platform (Illumina Inc, San Diego, CA, USA). The resulting reads were aligned to the reference genome (GRCh37/hg19) using the Burrows-Wheeler Alignment (BWA-0.5.10) [24]. Variants were referred to based on UnifiedGenotyper of the Genome Analysis Toolkit (GATK-1.6-11) and annotated with SnpEff-3.3 (Ensembl 73 database) [24]. The effect of protein-altering variants was assessed using different prediction tools: PolyPhen2 (<http://genetics.bwh.harvard.edu/pph2>) [25], SIFT (<http://sift.jcvi.org>) [26], MutationTaster [27], and Condel (<http://bbglab.irbbarcelona.org/fannsdb>) [28]. Deleterious variants, filtered according to inheritance (*de novo* heterozygous, double heterozygous, homozygous) were prioritized according to phenotype utilizing VarElect within GeneCards (PMID:22155609) [24] and confirmed with Sanger sequencing. The structural homology modelling of *KCNQ2* was performed with the automatic Swiss Model (<https://swissmodel.expasy.org/interactive>) using the target sequence of human *KCNQ2* (ACCESSION NP_742105) and the template file structure of human *KCNQ1* (6UZZ).

Mutagenesis and electrophysiological studies

Site-directed mutagenesis was generated by PCR amplification of human *KCNQ2* cDNA, using PCR-based Quikchange Site-Directed Mutagenesis (Stratagene). The p.Gly281Arg mutant cDNA clone was verified by DNA sequencing of the whole vector. CHO cells were maintained in Dulbecco's modified Eagle's medium (DMEM) supplemented with 2 mM glutamax (Gibco), 10% foetal bovine serum and antibiotics, and incubated at 37°C in 5% CO₂. Cells were seeded on poly-L-lysine-coated glass coverslips in a 24-multiwell plate, and transiently transfected with Transit LT1-Transfection Reagent (Mirus). The pIRES-CD8 vector was co-transfected as a transfection identification surface marker. Recordings were performed 40 hours after transfection, using the voltage-clamp configuration of the whole-cell patch-clamp technique, as previously described [29]. Transfected cells were visualized using anti-CD8 antibody-coated beads. Data were sampled at 5 kHz and low-pass filtered at 2 kHz (Axopatch200B amplifier with pclamp10 software and a 4-pole Bessel low pass filter, Molecular Devices). The patch pipettes were pulled



■ **Figure 1.** Brain imaging, electroencephalography and illustration of the p.Gly281Arg mutation. (A, B) Axial T2 brain MRI at four months (A) and 16 months (B) showing progressive atrophy and hypomyelination. C, D) Double banana montage of EEG recordings (70 mV amplitude). (C) High-amplitude disorganized background with abundant high-voltage multifocal spikes at three years of age, before treatment. (D) Low-amplitude asymmetric background (with left flattening) and right temporal slow spike-and-wave activity at five years of age, after treatment. (E) Illustration of the structure of the Kv7.2 channel; transmembrane domains 1-4 represent the voltage sensor domain and domains 5-6 form the pore; within the pore, the ion permeability filter motif is presented in red. (F) Structural modelling of glycine 281 (black arrow) in the selectivity filter of two opposed Kv7.2 subunits.

from borosilicate glass (Warner Instrument Corp) with a resistance of 3-7 M Ω , and filled with: 130 mM KCl, 5 mM Mg ATP, 5 mM EGTA, 10 mM HEPES, pH 7.3 (adjusted with KOH), and sucrose was added to adjust osmolarity to 290 mOsmol. The external solution contained: 140 mM NaCl, 4 mM KCl, 1.2 mM MgCl₂, 1.8 mM CaCl₂, 11 mM glucose, 5.5 mM HEPES, pH 7.3 (adjusted with NaOH), and sucrose was added to adjust osmolarity to 310 mOsmol. Data analysis was performed using the Clampfit program (pClamp10, Axon Instruments), Microsoft Excel and Prism 5.0 (GraphPad). Conductance (G) was calculated as $G = I / (V - V_{rev})$. G was then normalized to the maximal conductance. Activation curves were fitted to a single Boltzmann distribution according to $G/G_{max} = 1 / \{1 + \exp[(V_{50} - V) / s]\}$, where V_{50} is the voltage at which the current is half-activated and s is the slope factor. All data were expressed as mean \pm sem (standard error of the mean). Statistically significant differences were assessed by unpaired t test for two samples assuming unequal variances for comparing between wild-type (WT) and mutant channels, and by paired t-test of the means for comparing the effect of RTG before and after its application in the same cell. For electrophysiological experiments, RTG (HCl) was purchased from Alomone labs (Jerusalem).

Results

Case summary

The patient, a seven-year-old male, was born to healthy unrelated parents after an uneventful pregnancy. The mother reported increased uterine contractions, retrospectively attributed to presumed intrauterine seizures. Tonic-autonomic seizures, manifesting as tonic stiffening with hypoventilation and cyanosis, started on the first day of life, and were initially unresponsive to phenobarbitone at 20 mg/kg, and thereafter to phenytoin at 20 mg/kg. Over the next few months, in addition to tonic seizures, focal-onset clonic seizures (awareness unknown) also appeared, manifesting as episodes of jerking in alternate limbs,

lasting for a few minutes. Despite treatment with levetiracetam at 40 mg/kg, valproic acid at 30mg/kg, carbamazepine at 20 mg/kg, topiramate at 10 mg/kg and clonazepam at 0.1 mg/kg, he had hundreds of seizures per day. Towards one year of age, he was started on the ketogenic diet and oral diazepam was added unsuccessfully. At three years of age, during severe seizure exacerbation due to a febrile illness, potassium bromide at 40 mg/kg was added. Though a 20% reduction with bromide salts was observed, the drug was discontinued due to technical difficulties. Towards three years of age, he was on six antiseizure drugs (phenobarbitone, valproic acid, carbamazepine, topiramate, clonazepam, and oral diazepam) and the ketogenic diet, with no significant change in seizure frequency. Neurological examination at this age revealed severe hypotonia with absent deep tendon reflexes, optic atrophy and preserved head circumference. Brain MRI showed progressive hypomyelination and atrophy, raising a suspicion of a peroxisomal disorder (*figure 1A, B*). Initial EEG (performed at another institution; data unavailable) was reported as a burst-suppression pattern and evolved to a high-amplitude disorganized background with continuous multifocal spikes (*figure 1C*). The patient underwent extensive metabolic evaluation, which was negative. He never reached any developmental milestones, had blindness and was placed in an institution for infants with profound intellectual disability.

Molecular diagnosis

At three years of age, whole-exome sequencing revealed a heterozygous *de novo* pathogenic missense variant p.Gly281Arg in the *KCNQ2* gene, which encodes the Kv7.2 voltage-gated potassium channel. The pathogenic variant is located within the pore region, in a phylogenetically highly conserved motif, TVGYG, corresponding to the K⁺ ion selectivity filter (*figure 1E, F*; black arrow). The mutation substitutes glycine -a small, neutral amino acid- for the large, positively charged arginine, within the region responsible for binding K⁺ ions. The mutation is therefore predicted to give rise to a non-functional channel.

KCNQ2 channels are activated by the opener drug, RTG. A conserved tryptophan residue in the pore-forming S5 helix of RTG-sensitive KCNQ channels (KCNQ2 Trp236, KCNQ3 Trp265) is known to be essential for RTG effects. Since the binding site (Trp236) of the channel opener, RTG, is located in the S5 segment, downstream of the p.Gly281Arg mutation, we assumed that RTG would not be effective in increasing K⁺ current through the mutant channel, therefore treatment with this drug would be useless.

Electrophysiological studies

We introduced the p.Gly281Arg mutation into human KCNQ2 cDNA and transfected CHO cells. No functional current could be recorded in cells expressing homomeric KCNQ2^{pGly281Arg} (KCNQ2^{G281R}) channels (table 1). When the KCNQ2^{G281R} mutant was co-expressed at a 1/1 ratio with wild-type KCNQ2^{WT}, functional currents were observed. However, their densities were significantly much lower than the expected 50% for KCNQ2 homotetramers: at +30 mV, KCNQ2^{WT}/KCNQ2^{G281R}=24 ± 5 pA/pF (n=12) and KCNQ2^{WT/WT} homotetramers=153 ± 25 pA/pF (n=10); (unpaired t-test; p<0.01) (table 1, figure 2A-E). These data suggest that the pore mutant KCNQ2^{G281R} exerts a dominant-negative effect on the current density of KCNQ2^{WT} channels. The mutant subunit did not significantly affect the voltage dependence of activation: V₅₀ = -21.3 ± 0.7 mV, s = 6.6 ± 0.6 mV for KCNQ2^{WT}/KCNQ2^{G281R} (n=12) and V₅₀ = -24.8 ±

0.5 mV, s = 9.5 ± 0.5 mV for KCNQ2^{WT} (n=10) (table 1, figure 3A, B).

Next, we examined the impact of the mutant subunit on the allelic context of co-expression with the KCNQ3^{WT}, KCNQ2^{WT} and KCNQ2^{G281R} subunits at 1/1 ratio (each at 0.5 μg/well). Under these conditions, the current density for the mutant heterotetramer still remained lower than that of the wild-type: at +30 mV, KCNQ3^{WT}/KCNQ2^{WT}/KCNQ2^{G281R}=158 ± 62 pA/pF (n=12) vs. KCNQ2^{WT}/KCNQ3^{WT}=242 ± 67 pA/pF (n=12) (two-tailed unpaired t-test; p<0.05) (table 1, figure 2F-I). These results confirm the dominant-negative impact of the mutant subunit KCNQ2^{G281R}. The mutant did not significantly affect the voltage dependence of activation of the heteromeric complex: V₅₀ = -30.4 ± 0.7 mV, s = 7.6 ± 0.6 mV for KCNQ3^{WT}/KCNQ2^{WT}/KCNQ2^{G281R} (n=12) and V₅₀ = -25.4 ± 1.0 mV, s = 6.9 ± 0.9 mV for KCNQ2^{WT}/KCNQ3^{WT} (n=12) (table 1, figure 3C, D).

Thereafter, we examined the ability of RTG to enhance current generated by wild-type and mutant homotetramers and heterotetramers. RTG (5 μM) produced no effect on current with the non-functional homomeric KCNQ2^{G281R} channel, as expected (table 1), but exerted a potent opening activity with homomeric KCNQ2^{WT} channels by significantly increasing the current, 5 ± 0.8-fold, at -40 mV (figure 2A, 3E) (n = 10, two-tailed paired-test; p<0.01) and producing a -31.5-mV left-shift in voltage dependence of channel activation (n=10, two-tailed paired-test; p<0.01) (table 1, figure 3A). Despite the loss-of-function effect exerted by the

▼ **Table 1.** Current density and voltage-dependence parameters of KCNQ2^{WT} and mutant KCNQ2^{G281R} in different combinations of KCNQ3^{WT} with or without retigabine

Channel tetramer composition	Current density at +30 mV pA/pF	n	V ₅₀ (mV)	Slope s (mV)	n
KCNQ2 ^{WT}	153 ± 25	10	-24.8 ± 0.5	9.5 ± 0.5	10
KCNQ2 ^{WT} + RTG	207 ± 34	10	-56.3 ± 2.6	8.1 ± 1.5	10
KCNQ2 ^{G281R}	0 ± 0	7	ND	ND	7
KCNQ2 ^{G281R} +RTG	0 ± 0	7	ND	ND	7
KCNQ2 ^{WT} /KCNQ3 ^{WT}	242 ± 67	12	-25.4 ± 1.0	6.9 ± 0.9	12
KCNQ2 ^{WT} /KCNQ3 ^{WT} +RTG	164 ± 46	12	-49.5 ± 2.0	6.2 ± 1.7	12
KCNQ2 ^{WT} /KCNQ2 ^{G281R}	24 ± 5	12	-21.3 ± 0.7	6.6 ± 0.6	12
KCNQ2 ^{WT} /KCNQ2 ^{G281R} +RTG	24 ± 7	12	-38.0 ± 1.2	7.7 ± 1.1	12
KCNQ3 ^{WT} /KCNQ2 ^{WT} /KCNQ2 ^{G281R}	158 ± 62	12	-30.4 ± 0.7	7.6 ± 0.6	12
KCNQ3 ^{WT} /KCNQ2 ^{WT} /KCNQ2 ^{G281R} +RTG	159 ± 53	12	-51.3 ± 1.1	5.0 ± 1.0	12

n: number of cells; ND: not determined.

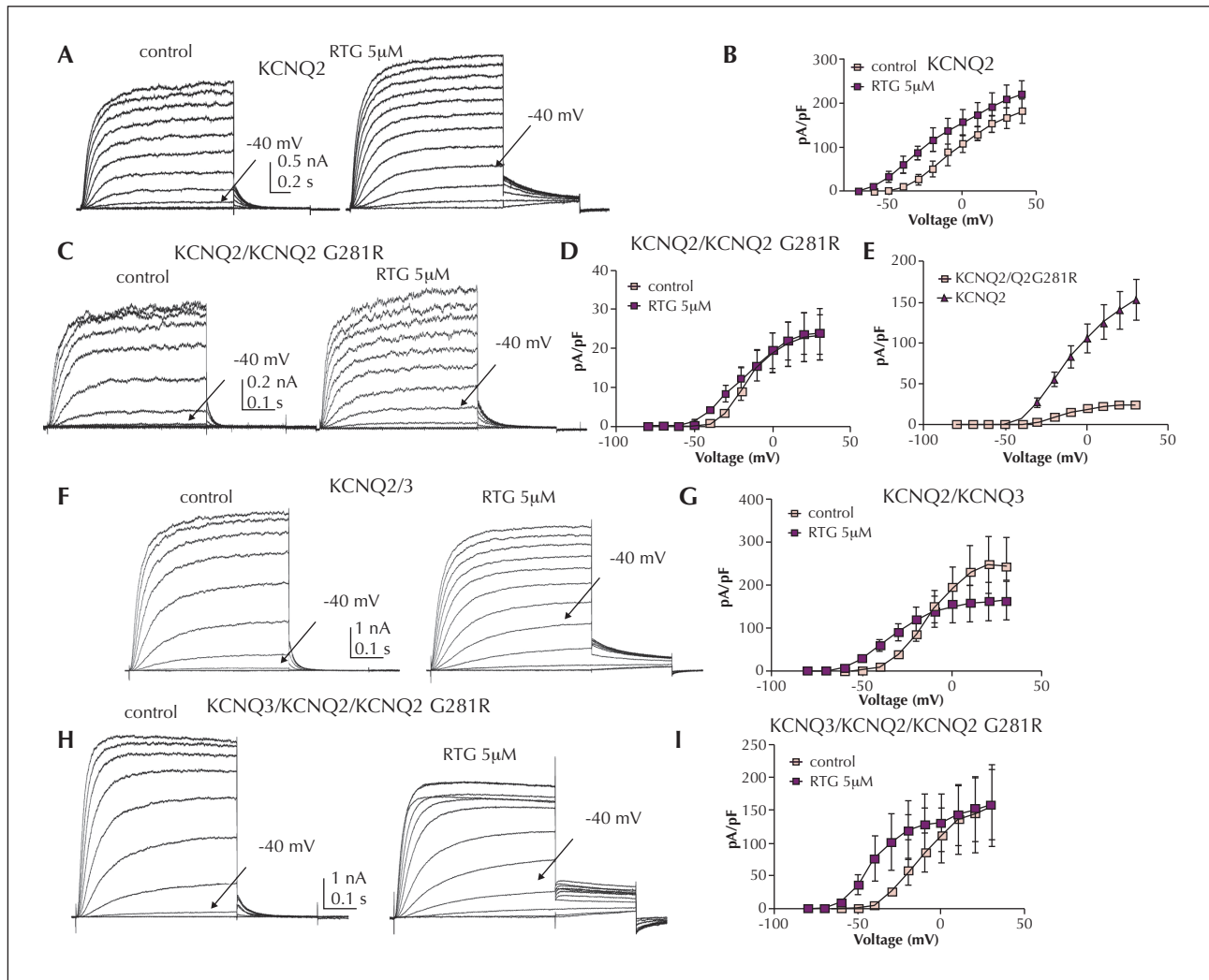


Figure 2. Potassium currents with mutant vs. wild-type heteromers (KCNQ2^{WT}/KCNQ3^{WT}, KCNQ2^{WT}/KCNQ2^{G281R} and KCNQ3^{WT}/KCNQ2^{WT}/KCNQ2^{G281R}) and effect of RTG. (A) Whole-cell currents with WT KCNQ2 in transfected CHO cells in the absence (control) and presence of 5 μM RTG (representative of 10 experiments). Cells were held at -90 mV and stepped for 0.5 seconds, from -80 mV to +30 mV, with 10 mV increments and repolarized at -60 mV. (B) Current density-voltage relationship for WT KCNQ2 in the absence (control) and presence of 5 μM RTG (*n* = 10). (C) Whole-cell currents with KCNQ2^{WT}/KCNQ2^{G281R} (representative of 12 experiments). (D, E) Current density-voltage relationship for KCNQ2^{WT}/KCNQ2^{G281R}; in the absence (control) and presence of 5 μM RTG (*n*=12) (D) as well as for WT KCNQ2 (*n*=12) and KCNQ2^{WT}/KCNQ2^{G281R} (*n*=10) (E). (F) Whole-cell currents with WT KCNQ2/KCNQ3 in the absence (control) and presence of 5 μM RTG (representative of 12 experiments). (G) Current density-voltage relationship for KCNQ2/KCNQ3 in the absence (control) and presence of 5 μM RTG (*n*=12). (H) Whole-cell currents for KCNQ3^{WT}/KCNQ2^{WT}/KCNQ2^{G281R} channels in the absence (control) and presence of 5 μM RTG (representative of 12 experiments). (I) Current density-voltage relationship for KCNQ3^{WT}/KCNQ2^{WT}/KCNQ2^{G281R} channels in the absence (control) and presence of 5 μM RTG.

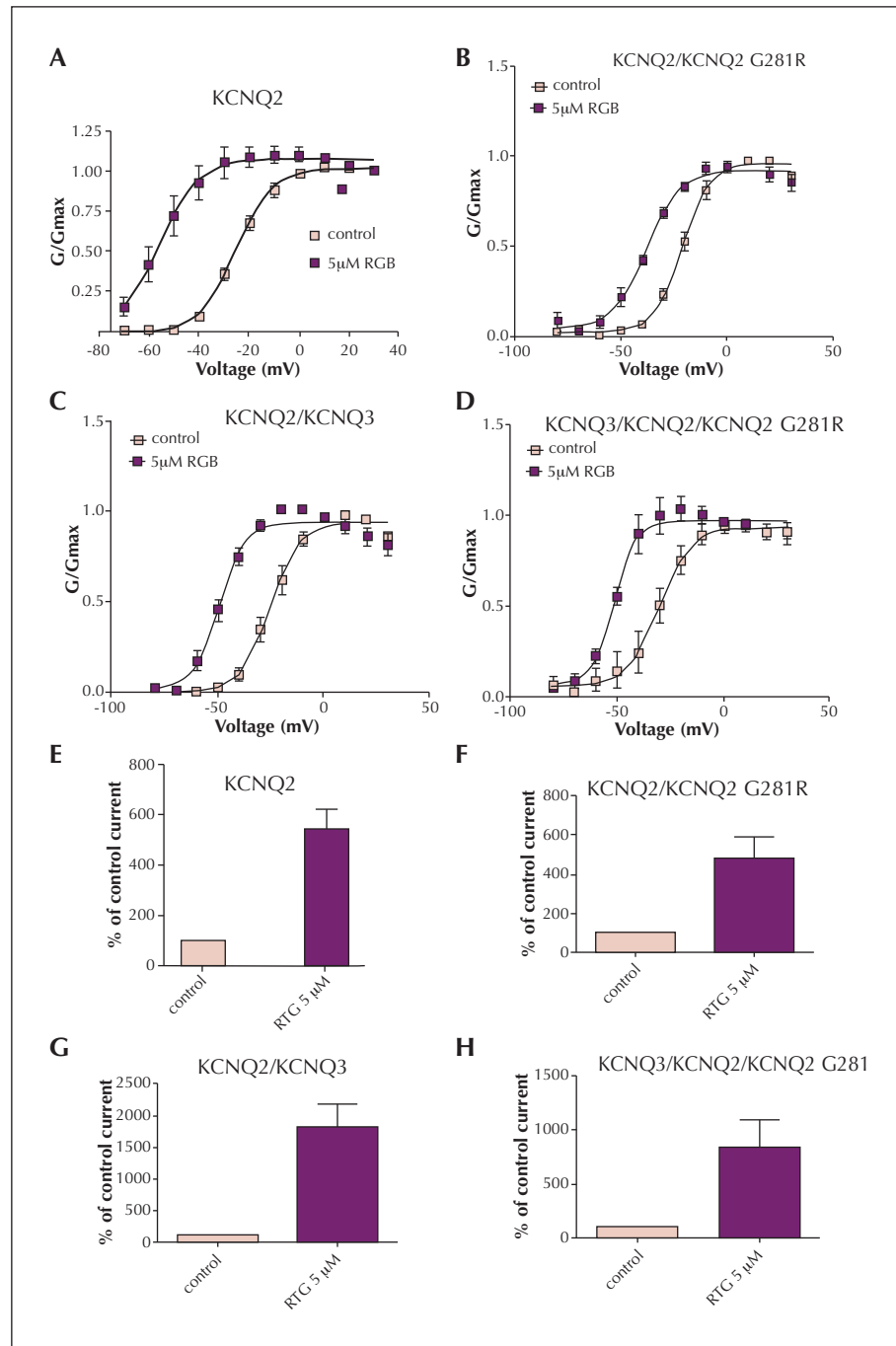


Figure 3. Effect of RTG on current amplitude and voltage dependence of activation with $KCNQ2^{WT}$, $KCNQ2^{WT}/KCNQ2^{G281R}$, $KCNQ2^{WT}/KCNQ3^{WT}$, and $KCNQ3^{WT}/KCNQ2^{WT}/KCNQ2^{G281R}$ channels. (A-D) Normalized conductances for $KCNQ2^{WT}$ (A), $KCNQ2^{WT}/KCNQ2^{G281R}$ (B), $KCNQ2^{WT}/KCNQ3^{WT}$ (C), and $KCNQ3^{WT}/KCNQ2^{WT}/KCNQ2^{G281R}$ (D) are plotted as a function of test voltage, in the absence and presence of 5 μ M RTG and fitted with a Boltzmann function. (E, H) The effect of 5 μ M RTG measured at +30 mV for $KCNQ2^{WT}$ (E), $KCNQ2^{WT}/KCNQ2^{G281R}$ (F), $KCNQ2^{WT}/KCNQ3^{WT}$ (G), and $KCNQ3^{WT}/KCNQ2^{WT}/KCNQ2^{G281R}$ (H) and expressed as percentage of control.

mutated subunit KCNQ2^{G281}, RTG (5 μ M) produced a significant hyperpolarizing shift of -16.7 mV and -20.9 mV, respectively, in the voltage dependence of activation of KCNQ2^{WT}/KCNQ2^{G281R} and KCNQ3^{WT}/KCNQ2^{WT}/KCNQ2^{G281R} channels ($n=12$, two-tailed paired t-test; $p<0.01$) (table 1, figure 3B, D). RTG also increased the respective currents by 4.8 ± 1 -fold and 8.4 ± 2.6 -fold at -40 mV ($n = 12$, two-tailed paired t-test; $p<0.01$) (figure 3F, H). For comparison, RTG (5 μ M) produced a left-shift of -24.1 mV in the voltage dependence of activation of KCNQ2^{WT}/KCNQ3^{WT} channels (table 1, figure 3C) ($V_{50} = -25.4 \pm 1.0$ mV, $s = 6.9 \pm 0.9$ mV [$n=12$] and $V_{50} = -49.5 \pm 2.0$ mV, $s = 6.2 \pm 1.7$ mV [$n=12$], in the absence and presence of RTG, respectively) ($n=12$, two-tailed paired t-test; $p<0.005$). At -40 mV, RTG increased the current with KCNQ2^{WT}/KCNQ3^{WT} by 18.3 ± 3.3 -fold ($n=12$, two-tailed paired t-test; $p<0.001$) (figure 3D).

Treatment

Ensuing the positive effect that we observed on patch-clamp analysis, at four years of age, treatment with RTG (Trobal[®]) was instituted off-label, according to approval for compassionate use, since the drug was not approved for treatment in this age group. The dosage was gradually increased over three weeks, up to 15 mg/kg (50 mg*3). There was no existing formulation for children, hence tablets were crushed and administered per gastrostomy tube. Blood levels could not be monitored, since there are no available clinical tests. Three months into therapy, seizure burden decreased from about 100/day to 4-5/day (over 90% reduction). We reduced concomitant drug therapy from four antiepileptic drugs (phenobarbitone, topiramate, clonazepam, and oral diazepam) and the ketogenic diet, to two antiepileptic drugs (topiramate and phenobarbitone) and stopped the ketogenic diet. EEG recording (figure 1D) showed improved background and decreased epileptiform activity. Though seizure burden decreased significantly, there were no developmental milestones acquired nor improvement in visual ability. On neurological examination, there was a subjective impression of improvement in general well-being, alertness and muscle tone. There were no perceived side effects, such as blue skin discolouration or urinary retention.

Unfortunately, after two years of treatment, Trobal[®] was withdrawn from the market due to side effects (<https://www.epilepsysociety.org.uk/news/epilepsy-drug-trobal-RTG-to-be-discontinued-14-09-2016#>. WdnQn8IUUnIU). Two months after withdrawal, there was a 50% increase in seizure frequency (from 10 seizures/day to 20 seizures/day). No EEG recording was

performed after RTG termination. Partial improvement in seizure control was achieved by adding the sodium channel blocker, lacosamide.

Discussion

Pathogenic variants in the KCNQ2 gene, a subunit encoding for the voltage-gated potassium channel-Kv7.2, cause neonatal epilepsies with variable outcome [10, 30-32] (RIKEE database: www.rikee.org). Mostly, genotype-phenotype correlations are described based on clinical presentation, without systematic support from electrophysiological data. However, several patch-clamp studies have established a correlation between clinical severity and degree of functional impairment, especially for mutations located in regions crucial for channel functioning [12-16].

Kv7.2, similar to other voltage-gated potassium channels, comprises a voltage sensor, a pore and a S4-S5 linker, which couples voltage sensor movement to the passage of K⁺ ions through the pore [1]. The K⁺ channel pore comprises a narrow ion passage, highly evolutionarily conserved from bacteria to humans, which confers selectivity to K⁺ ions in the channel [1]. Mutations located within the K⁺ selectivity filter have been occasionally described in the literature in children with epilepsy [30, 31, 33-35].

In this study, we describe a seven-year-old boy with early epileptic encephalopathy (Ohtahara syndrome) bearing a missense pathogenic variant (p.Gly281Arg) located within the KCNQ2 K⁺-selectivity filter. We predicted this mutation to be highly deleterious to channel function, since the mutation leads to a substitution of a small, neutral amino acid (glycine) by a large positively charged amino acid (arginine) within the narrowest region of the pore responsible for passage of the positively charged K⁺ ions (figure 1E). Although, we cannot totally exclude issues associated with trafficking, we suggest that this pore mutation results in a non-functional subunit, in which the selective coordination of dehydrated K⁺ ions, exerted by oxygen atoms from the main carbonyl chain of amino acids located in the filter (GYG), is not achieved, leading to pore collapse. Indeed, the clinical disease of this infant was extremely severe, with morbidity starting already *in utero*, hypomyelination on MRI resembling a peroxisomal disorder, and pharmacoresistant seizures which responded to low-dose RTG (15 mg/kg). Located in a highly conserved motif, the same variant has been described previously several times. Weckhuysen *et al.* briefly described two patients bearing the same mutation; in particular, Patient M in this study [30] presented with very similar symptoms to those of our patient, with intrauterine

seizures, hypomyelination and a positive response to high-dose RTG at 40m g/kg. In a study by Olson *et al.*, two of 33 patients with early-onset epileptic encephalopathy and burst-suppression harbored the p. Gly281Arg mutation [34]. Recently, Gomes-Perez *et al.* described a patient with severe pharmacoresistant early-onset epileptic encephalopathy who passed away at the age of 14 months, but was not treated with RTG [35]). Pisano *et al.* described an infant with a milder neonatal epileptic encephalopathy associated with a different amino acid substitution at the same site, p.Gly281Trp; seizures were responsive to early treatment with sodium channel blockers [31]. The better clinical outcome of this patient compared to that of ours may have been due to a less extreme dominant-negative effect of the p.Gly281Trp variant. The aim of this study was to characterize the biophysical effects of this predicted highly pathogenic variant, in order to direct potential targeted therapy with RTG. As expected, no functional current could be recorded in cells expressing homomeric KCNQ2^{G281R}, indicating a complete loss of function. However, co-expression with the wild-type subunit, as a heterodimer or heterotetramer, revealed an additive dominant-negative effect on current density. Our data is in line with that of Peters *et al.* who demonstrated that p.Gly279Ser mutation in the filter motif in an animal knock-in model caused marked dominant-negative current suppression [36]. A recent study by Comis-Peres *et al.* revealed similar results with a dominant-negative effect in a child with the same p.Gly281Arg variant [35]. In this context, we suggest that the dominant-negative nature of the pore mutation, p.Gly281Arg, implies an ability of the non-functional subunit to randomly associate with normal subunits KCNQ3^{WT} or KCNQ2^{WT} to form various heterotetramers.

Prior to starting targeted therapy, we doubted that channel openers would be effective due to the non-functional nature of the -mutant channel and the dominant-negative effect on heteromers. Although RTG had no effect on the homomeric mutant KCNQ2^{G281R}, RTG produced a significant increase in current with heteromers (KCNQ2^{WT}/KCNQ2^{G281R} and KCNQ3^{WT}/KCNQ2^{WT}/KCNQ2^{G281R}) (table 1, figure 3). Our results provide a plausible functional explanation for the positive outcome of seizures with RTG treatment in our patient and a patient from the study of Weckhuysen *et al.* [25]. Regrettably, in our study, treatment was started after four years of age, and despite a 90% reduction in seizure frequency, no significant improvement was achieved in developmental milestones. We can only speculate that with treatment instituted in the first year of life, we might have been able to significantly improve developmental outcome, as communicated by Pisano *et al.* [31].

Unfortunately, RTG (Trobal[®]) has been recently discontinued in 2017 (<https://www.epilepsysociety.org.uk/news/epilepsy-drug-trobal-RTG-to-be-discontinued-14-09-2016#.WdnQn8IUUnIU>) due to safety issues as it may cause a blue discolouration of the skin and eye abnormalities, as well as sedative effects. A Phase 3 trial, repurposing RTG (XEN496) as a targeted therapy for children with KCNQ2-related developmental and epileptic encephalopathy, has recently started (ClinicalTrials.gov: NCT04639310). In addition, promising RTG analogues with improved safety properties are also currently under active investigation [37].

Kv7 openers are targeted therapies in KCNQ2-related epilepsies. Patch-clamp analysis should not be a requirement prior to institution of therapy, but can be very useful in predicting response to therapy. One should be aware that whilst RTG might control seizures in cases with loss-of-function mutations, seizure exacerbation is to be expected with gain-of-function mutations [11]. However, electrophysiological studies are time-consuming and expensive, prompting future development of alternative methods (e.g. computerized functional modelling, automated patch-clamp analysis, and machine-learning algorithms based on large databases) to predict the effect of ion channel mutations. ■

Supplementary material.

Summary slides accompanying the manuscript are available at www.epilepticdisorders.com.

Disclosures.

None of the authors have any conflicts of interest or disclosure to declare

References

- Cooper EC. Potassium channels (including KCNQ) and epilepsy. In : Noebels JL, Avoli M, Rogawski MA, Olsen RW, Delgado-Escueta AV, (eds). *Jasper's basic mechanisms of the epilepsies*. Bethesda (MD): National Center for Biotechnology Information (US).
- Cooper EC, Harrington E, Jan YN, Jan LY. M channel KCNQ2 subunits are localized to key sites for control of neuronal network oscillations and synchronization in mouse brain. *J Neurosci* 2001; 21(24): 9529-40.
- Cooper EC. Potassium channels: how genetic studies of epileptic syndromes open paths to new therapeutic targets and drugs. *Epilepsia* 2001; 42(Suppl 5): 49-54.
- Shah MM, Migliore M, Valencia I, Cooper EC, Brown DA. Functional significance of axonal Kv7 channels in hippocampal pyramidal neurons. *Proc Natl Acad Sci U S A* 2008; 105(22): 7869-74.

5. Shah M, Mistry M, Marsh SJ, Brown DA, Delmas P. Molecular correlates of the M-current in cultured rat hippocampal neurons. *J Physiol* 2002; 544(Pt 1): 29-37.
6. Delmas P, Brown DA. Pathways modulating neural KCNQ/M (Kv7) potassium channels. *Nat Rev Neurosci* 2005; 6(11): 850-62.
7. Jentsch TJ. Neuronal KCNQ potassium channels: physiology and role in disease. *Nat Rev Neurosci* 2000; 1(1): 21-30.
8. Biervert C, Schroeder BC, Kubisch C, Berkovic SF, Propping P, Jentsch TJ, et al. A potassium channel mutation in neonatal human epilepsy. *Science* 1998; 279(5349): 403-6.
9. Singh NA, Charlier C, Stauffer D, DuPont BR, Leach RJ, Melis R, et al. A novel potassium channel gene, KCNQ2, is mutated in an inherited epilepsy of newborns. *Nat Genet* 1998; 18(1): 25-9.
10. Weckhuysen S, Mandelstam S, Suls A, Audenaert D, Deconinck T, Claes LR, et al. KCNQ2 encephalopathy: emerging phenotype of a neonatal epileptic encephalopathy. *Ann Neurol* 2012; 71(1): 15-25.
11. Millichap JJ, Park KL, Tsuchida T, Ben-Zeev B, Carmant L, Flamini R, et al. KCNQ2 encephalopathy: features, mutational hot spots, and ezogabine treatment of 11 patients. *Neurol Genet* 2016; 2(5): e96.
12. Miceli F, Soldovieri MV, Ambrosino P, Barrese V, Migliore M, Cilio MR, et al. Genotype-phenotype correlations in neonatal epilepsies caused by mutations in the voltage sensor of K(v)7.2 potassium channel subunits. *Proc Natl Acad Sci U S A* 2013; 110(11): 4386-91.
13. Dedek K, Kunath B, Kananura C, Reuner U, Jentsch TJ, Steinlein OK. Myokymia and neonatal epilepsy caused by a mutation in the voltage sensor of the KCNQ2 K+ channel. *Proc Natl Acad Sci U S A* 2001; 98(21): 12272-7.
14. Castaldo P, del Giudice EM, Coppola G, Pascotto A, Annunziato L, Tagliatela M. Benign familial neonatal convulsions caused by altered gating of KCNQ2/KCNQ3 potassium channels. *J Neurosci* 2002; 22(2): Rc199.
15. Lee IC, Yang JJ, Liang JS, Chang TM, Li SY. KCNQ2-associated neonatal epilepsy: phenotype might correlate with genotype. *J Child Neurol* 2017; 32(8): 704-11.
16. Hunter J, Maljevic S, Shankar A, Siegel A, Weissman B, Holt P, et al. Subthreshold changes of voltage-dependent activation of the K(V)7.2 channel in neonatal epilepsy. *Neurobiol Dis* 2006; 24(1): 194-201.
17. Millichap JJ, Miceli F, De Maria M, Keator C, Joshi N, Tran B, et al. Infantile spasms and encephalopathy without preceding neonatal seizures caused by KCNQ2 R198Q, a gain-of-function variant. *Epilepsia* 2017; 58(1): e10-5.
18. Miceli F, Soldovieri MV, Ambrosino P, De Maria M, Migliore M, Migliore R, et al. Early-onset epileptic encephalopathy caused by gain-of-function mutations in the voltage sensor of Kv7.2 and Kv7.3 potassium channel subunits. *J Neurosci* 2015; 35(9): 3782-93.
19. Gunthorpe MJ, Large CH, Sankar R. The mechanism of action of retigabine (ezogabine), a first-in-class K+ channel opener for the treatment of epilepsy. *Epilepsia* 2012; 53(3): 412-24.
20. Blackburn-Munro G, Dalby-Brown W, Mirza NR, Mikkelsen JD, Blackburn-Munro RE. Retigabine: chemical synthesis to clinical application. *CNS Drug Rev* 2005; 11(1): 1-20.
21. Barrese V, Miceli F, Soldovieri MV, Ambrosino P, Iannotti FA, Cilio MR, et al. Neuronal potassium channel openers in the management of epilepsy: role and potential of retigabine. *Clin Pharmacol* 2010; 2: 225-36.
22. Ihara Y, Tomonoh Y, Deshimaru M, Zhang B, Uchida T, Ishii A, et al. Retigabine, a Kv7.2/Kv7.3-channel opener, attenuates drug-induced seizures in knock-in mice harboring Kcnq2 mutations. *PLoS One* 2016; 11(2): e0150095.
23. Claes LR, Ceulemans B, Audenaert D, Deprez L, Jansen A, Hasaerts D, et al. De novo KCNQ2 mutations in patients with benign neonatal seizures. *Neurology* 2004; 63(11): 2155-8.
24. Zhu X, Petrovski S, Xie P, Ruzzo EK, Lu YF, McSweeney KM, et al. Whole-exome sequencing in undiagnosed genetic diseases: interpreting 119 trios. *Genet Med* 2015; 17(10): 774-81.
25. Adzhubei IA, Schmidt S, Peshkin L, Ramensky VE, Gerasimova A, Bork P, et al. A method and server for predicting damaging missense mutations. *Nat Methods* 2010; 7(4): 248-9.
26. Kumar P, Henikoff S, Ng PC. Predicting the effects of coding non-synonymous variants on protein function using the SIFT algorithm. *Nat Protoc* 2009; 4(7): 1073-81.
27. Schwarz JM, Cooper DN, Schuelke M, Seelow D. MutationTaster2: mutation prediction for the deep-sequencing age. *Nat Methods* 2014; 11(4): 361-2.
28. Gonzalez-Perez A, Lopez-Bigas N. Improving the assessment of the outcome of nonsynonymous SNVs with a consensus deleteriousness score, Condel. *Am J Hum Genet* 2011; 88(4): 440-9.
29. Peretz A, Pell L, Gofman Y, Haitin Y, Shamgar L, Patrich E, et al. Targeting the voltage sensor of Kv7.2 voltage-gated K+ channels with a new gating-modifier. *Proc Natl Acad Sci U S A* 2010; 107(35): 15637-42.
30. Weckhuysen S, Ivanovic V, Hendrickx R, Van Coster R, Hjalgrim H, Moller RS, et al. Extending the KCNQ2 encephalopathy spectrum: clinical and neuroimaging findings in 17 patients. *Neurology* 2013; 81(19): 1697-703.
31. Pisano T, Numis AL, Heavin SB, Weckhuysen S, Angriman M, Suls A, et al. Early and effective treatment of KCNQ2 encephalopathy. *Epilepsia* 2015; 56(5): 685-91.
32. Kato M, Yamagata T, Kubota M, Arai H, Yamashita S, Nakagawa T, et al. Clinical spectrum of early onset epileptic encephalopathies caused by KCNQ2 mutation. *Epilepsia* 2013; 54(7): 1282-7.
33. Milh M, Lacoste C, Cacciagli P, Abidi A, Sutura-Sardo J, Tzelepis I, et al. Variable clinical expression in patients with mosaicism for KCNQ2 mutations. *Am J Med Genet A* 2015; 167a(10): 2314-8.
34. Olson HE, Kelly M, LaCoursiere CM, Pinsky R, Tambunan D, Shain C, et al. Genetics and genotype-phenotype correlations in early onset epileptic encephalopathy with burst suppression. *Ann Neurol* 2017; 81(3): 419-29.

35. Gomis-Perez C, Urrutia J, Marce-Grau A, Malo C, Lopez-Laso E, Felipe-Rucian A, *et al.* Homomeric Kv7.2 current suppression is a common feature in KCNQ2 epileptic encephalopathy. *Epilepsia* 2019; 60(1): 139-48.
36. Peters HC, Hu H, Pongs O, Storm JF, Isbrandt D. Conditional transgenic suppression of M channels in mouse brain reveals functions in neuronal excitability, resonance and behavior. *Nat Neurosci* 2005; 8(1): 51-60.
37. Davoren JE, Claffey MM, Snow SL, Reese MR, Arora G, Butler CR, *et al.* Discovery of a novel Kv7 channel opener as a treatment for epilepsy. *Bioorg Med Chem Lett* 2015; 25(21): 4941-4.

TEST YOURSELF

- (1) Are functional studies important in predicting the effect of potassium channel openers in cases with *KCNQ2* mutation?
- (2) Are potassium channel openers useful in cases with *KCNQ2* complete loss-of-function mutations (non-conducting channels)?
- (3) Does age at onset of treatment affect outcome?

Note: Reading the manuscript provides an answer to all questions. Correct answers may be accessed on the website, www.epilepticdisorders.com.
